Ocean Systems Engineering, *Vol. 14, No. 3 (2024) 301-314*
https://doi.org/10.12989/ose.2024.14.3.301

Analytic solution for flat-plate under a free surface with finite depth effects

Sakir Bal*

Department of Naval Architecture and Marine Engineering, Istanbul Technical University, Istanbul, Turkey

(Received July 3, 2024, Revised September 3, 2024, Accepted September 16, 2024)

Abstract. In this study, the lift coefficient and wave deformations for a two-dimensional flat-plate in non-cavitating condition were computed using a closed-form (analytic) solution. This plate moves at a constant speed beneath a free surface in water of finite depth. The model represents the flat-plate using a lumped vortex element within the constraints of potential flow theory. The kinematic and dynamic free surface conditions were combined and linearized. This linearized free surface condition was then applied to get the total velocity potential. The method of images was utilized to account for the effects of finite depth in the calculations. The lift coefficient of the flat-plate and wave elevations on the free surface were calculated using the closed-form solution. The lift coefficients derived from the present analytic solution were validated by comparing them with Plotkin's method in the case of deep water. Wave elevations were also compared with those obtained from a numerical method. A comprehensive discussion on the impact of Froude number, submergence depth of flat-plate from the calm free surface, the angle of attack and the depths of finite bottom on the results – namely, lift coefficients and free surface deformations – is provided.

Keywords: finite depth; flat-plate; free surface; lumped vortex element; method of images

1. Introduction

The hydrodynamic characteristics of two-dimensional non-cavitating (or even cavitating) hydrofoils, moving at a constant speed beneath a free surface have been extensively studied in previous studies (Bai and Han 1994, Bal *et al*. 2001, Faltinsen and Semenov 2008, Bal 2011, Chen 2012). More advanced methods have also been developed to solve this issue with contemporary methods (Gretton *et al*. 2010, Roohi *et al.* 2013). However, to the best of author's knowledge, no study has been addressed the effects of both free surface and finite bottom on non-cavitating flat-plates, represented by lumped vortex elements. The current study aims to bridge this gap by developing an analytic (closed-form) solution specifically addressing this problem.

Historically, various numerical methods were developed to analyze flows around cavitating and non-cavitating hydrofoils moving under a free surface. The Boundary Element Methods were (and still are) known as their computationally efficient and robust models to solve this problem under the conditions and restrictions of potential flow theory. For example, a previous study numerically investigated two-dimensional cavitating and/or non-cavitating hydrofoils moving steadily under a

*Corresponding author, Ph.D., E-mail: sbal@itu.edu.tr

http://www.techno-press.org/?journal=ose&subpage=7 ISSN: 2093-6702 (Print), 2093-677X (Online)

free surface using an iterative boundary element method (Bal and Kinnas 2002, Bal 2011). An integral equation was derived by applying Green's theorem to the hydrofoil surface and free surface, subsequently divided the full problem into two parts (cavitating hydrofoil and free surface). These two parts were solved separately with iterative consideration of their effects. The iterative method was applied before for hydrofoils placed within a cavitation tunnel (Choi and Kinnas, 1998) and later modified and extended for the surface-piercing hydrofoils and ships (Bal 2008). It was also applied for both two- and three-dimensional wings flying over free water surface (Bal 2016). A novel adjoint optimization method, based on a boundary element technique, was proposed for analyzing partially cavitating hydrofoils moving at a constant speed beneath the free surface (Anevlavi and Belibassakis 2022, Anevlavi and Belibassakis 2021, Vrinos *et al*. 2021). In a recent study, the effects of free surface on the flow field around a line sink were computed analytically for small Froude numbers and numerically for nonlinear problems (Mansoor *et al.* 2022). A comparison of Neumann-Kelvin (linearized free surface condition) and Rankine source (nonlinear free surface condition) methods was done for wave drag calculations of ships in (Yu and Falzarano 2017). Advanced methods such as CFD (Karim *et al.* 2014, Celik *et al*. 2014) also offer realistic solutions but come with higher computational costs in terms of computational memory and time. In contrast, lumped vortex element serves as a simplified representation of flat-plate (Katz and Plotkin 2001), inherently satisfying the Kutta condition at the trailing edge of flat-plate and providing an exact solution (Katz 2019). This representation can be extended to include thin cambered hydrofoils and multi-element lifting bodies, as well as applied to bi-foil and tandem hydrofoils. The hydrodynamic characteristics of cavitating flat-plate were also studied in the previous work (Kinnas 1992). The slotted cavitating hydrofoil design for an amphibious aircraft was examined by a numerical method in (Conesa and Liem 2020). In this study, it was aimed to minimize the cavitation on hydrofoil surface. On the other hand, the finite depth effects on hydrodynamic motion and load response on offshore structures were considered by a numerical method of the corresponding Green function in (Xie *et al*. 2017).

In this study, a non-cavitating flat-plate moving steadily under a free surface in water of finite depth is modeled using a lumped vortex element. Closed-form solutions for the lift coefficient and free surface deformation are developed based on these equations. Section 2 explains the mathematical modelling, including the governing equation and boundary conditions. Section 3 presents the solution using the method of images. In Section 4, the analytical results are compared with those obtained from other numerical methods, followed by concluding remarks in Section 5.

2. Mathematical modelling

A boundary value problem is formulated to address the steady uniform flow passing a two-dimensional non-dimensional flat-plate located beneath a free surface in water of finite depth. The flow field is assumed to be incompressible, inviscid and irrotational, thereby applying potential flow theory. The x-axis is oriented positively in the direction of uniform inflow (U), and the z-axis is positive upwards as illustrated in Fig. 1. The flat-plate is positioned beneath the calm free surface at $z = -h$. The governing equation dictates that the perturbation potential, ϕ and the total potential, Φ ($= Ux + \phi$) must satisfy the Laplace's equation (continuity equation) within the fluid domain

$$\nabla^2\Phi(x,z) = \nabla^2\phi(x,z) = 0 \tag{1}$$

Additionally, the perturbation potential function ϕ, must satisfy the following boundary conditions:

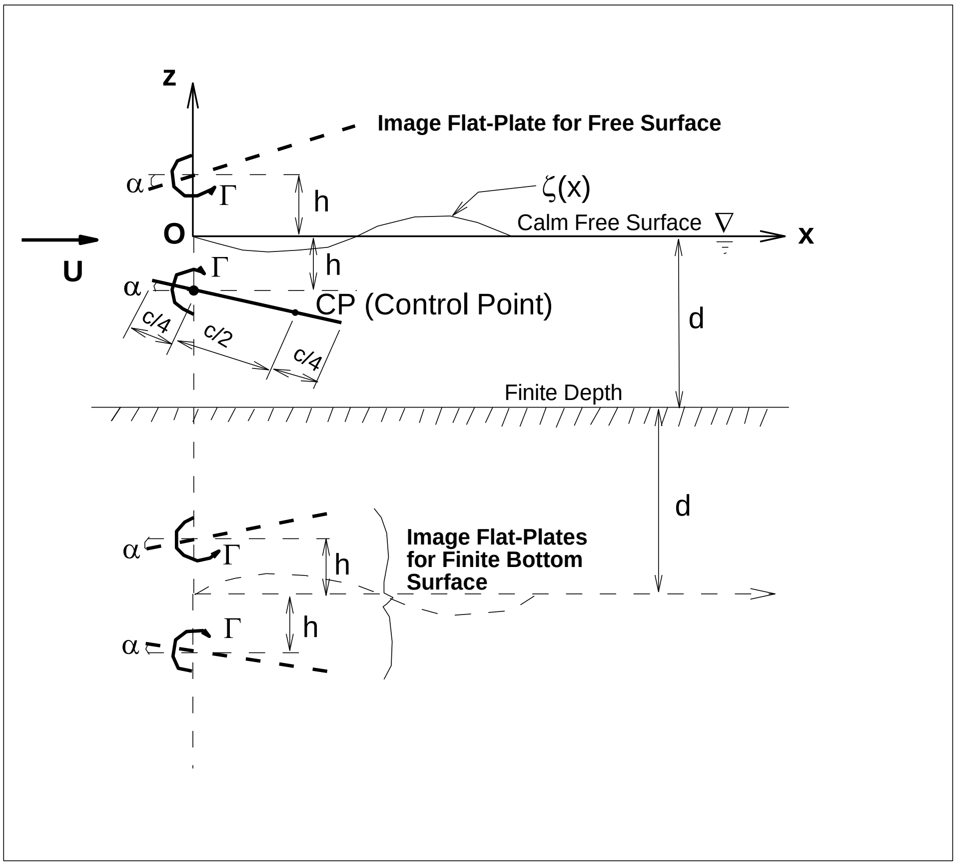

Fig. 1 Definition of problem, lumped vortex element, its images and coordinate system

<u>1-) Linearized free surface condition:</u> The kinematic free surface condition which means that the fluid particles should follow the free surface, must be satisfied

$$\frac{DF(x,z)}{Dt} = 0 \quad \text{on} \quad z = \zeta(x) \tag{2}$$

Here, F(x,z)=z-ζ(x), see Fig. 1. The dynamic free surface condition which means that the pressure on the free surface should be equal to atmospheric pressure, must also be satisfied. After applying Bernoulli's equation on the free surface, the following equation can be written

$$\frac{1}{2}[(\nabla\phi + U)^2 - U^2] + g\zeta = 0 \quad \text{on} \quad z = \zeta(x) \tag{3}$$

When the Eqs. (2) and (3) are combined and made linearized, the following free surface equation can be written:

$$\frac{\partial^2\phi}{\partial x^2} + k_0\frac{\partial\phi}{\partial z} = 0 \quad \text{on} \quad z = 0 \tag{4}$$

where, $k_0=g/U^2$ is the wave number, and g is the gravitational acceleration. The corresponding linearized wave elevation, derived from the Bernoulli equation, Eq. (3), is expressed as

$$\zeta = -\frac{U}{g}\frac{\partial \phi}{\partial x} \tag{5}$$

2-) Radiation condition: This condition prevents upstream waves. The potential function must satisfy the following equations:

$$\lim_{x\to-\infty} \phi \to 0 \quad \text{and} \quad \lim_{x\to\infty} \phi \to M \tag{6}$$

Here M is a finite number.

3-) Finite depth condition: The normal derivative of perturbation potential on the surface of finite bottom should be zero

$$\frac{\partial \phi}{\partial z} = 0 \quad \text{on} \quad z = -d \tag{7}$$

Other conditions, the Kutta condition and kinematic condition on flat-plate, are explained below.

3. Method of solution

The flat-plate has been represented using a lumped vortex element (Katz and Plotkin 2001). In this model, the cumulative effect of distributed vortices on the flat-plate is replaced by a simple single vortex with strength Γ, placed at the quarter-chord point and the kinematic boundary condition (zero normal velocity condition) is satisfied at the three-quarter chord point (Katz 2019). The Kutta condition at the trailing edge of flat-plate is automatically fulfilled within this model (Katz and Plotkin 2001). The method of images was employed to address the linearized free surface condition. First, the study focuses on the non-cavitating flow case without finite depth effects. The potential function ϕ_1 for a single vortex with strength Γ, located at z = - h is expressed as follows (Katz and Plotkin 2001)

$$\phi_1(x, z) = -\frac{\Gamma}{2\pi}\tan^{-1}\left(\frac{z+h}{x}\right) \tag{8}$$

By utilizing the following integral equation (Gradshteyn and Ryzhik 1965):

$$\int_0^\infty e^{-k(z+h)} \sin(kx)\, dk = \frac{x}{x^2+(z+h)^2} \tag{9}$$

and taking the derivative of Eq. (8) with respect to z, ϕ_1 can be re-written as:

$$\phi_1(x, z) = \frac{\Gamma}{2\pi}\int_0^\infty \frac{e^{-k(z+h)}\sin(kx)}{k} dk \tag{10}$$

It is assumed that the perturbation potential is the summation of $\phi(x, z) = \phi_1 + \phi_2 + \phi_3$. Here, ϕ_2 is the potential function due to the mirror image of single vortex with the same strength **Γ** and in the opposite direction of rotation, and ϕ_3 is the gravitational wave potential and can be calculated by using free surface condition, Eq. (4), as follows

$$\phi_2(x, z) = -\frac{\Gamma}{2\pi}\tan^{-1}\left(\frac{h-z}{x}\right) = \frac{\Gamma}{2\pi}\int_0^\infty \frac{e^{-k(h-z)}\sin(kx)}{k} dk \tag{11}$$

$$\phi_3(x,z) = -\frac{\Gamma}{\pi}\int_0^{\infty}\frac{e^{-k(h-z)}\sin(kx)}{k-k_0}dk \tag{12}$$

For the evaluation of definite integral I, in Eq. (12), the method of solution given in (Hess and Smith 1966) has been adopted here. The integral, "I" can now be written as

$$I = \int_0^{\infty}\frac{e^{-k(h-z)}\sin(kx)}{k-k_0}dk = \frac{b.c-a.d}{c^2+d^2} + C\pi e^{-k_0(h-z)}\cos(k_0 x) \tag{13}$$

Here, C is two (2) for $x\rightarrow+\infty$ and it is zero (0) for $x\rightarrow-\infty$, ensuring satisfaction of the radiation condition given in Eq. (6). The calculated a, b, c and d coefficients are provided in the Appendix (Hess and Smith1966).

Now, if the kinematic boundary condition (zero normal velocity) is applied at three-quarter chord point of flat-plate, the following equation holds

$$\frac{\partial\phi\left(x=\frac{c}{2}\cos\alpha,\, z=-h-\frac{c}{2}\sin\alpha\right)}{\partial z} = -U(\sin\alpha)(\cos\alpha) \tag{14}$$

and if the circulation value for lumped vortex element in an unbounded flow domain (no free surface case) $\boldsymbol{\Gamma}_{\infty}$ is utilized

$$\Gamma_{\infty} = \pi U c(\sin\alpha) \tag{15}$$

the following equation for circulation ratio can be obtained as

$$\frac{\Gamma}{\Gamma_{\infty}} = \left(\frac{\cos\alpha}{c}\right)\left[\frac{1}{2}\frac{x}{x^2+(z+h)^2} + \frac{1}{2}\frac{x}{x^2+(h-z)^2} + k_0 I\right]^{-1} \text{at}\left(x=\frac{c}{2}\cos\alpha, z=-h-\frac{c}{2}\sin\alpha\right) \tag{16}$$

Note that

$$\frac{\Gamma}{\Gamma_{\infty}} = \frac{C_L}{C_{L\infty}} \tag{17}$$

Here, C_L is the lift coefficient of flat-plate with free surface effect and $C_{L\infty}$ is the lift coefficient of flat-plate in unbounded flow domain (no free surface effect), and $C_{L\infty}=2\pi(\sin\alpha)$. The lift coefficient is defined as follows

$$C_L = \frac{L}{\frac{1}{2}\rho U^2 c} \tag{18}$$

In this equation, L represents the lift force of flat-plate.

Furthermore, the wave elevation on the free surface can be calculated from Eq. (5) as follows

$$\frac{\zeta(x; z=0)}{c} = \left(\frac{(\sin\alpha)(\cos\alpha)}{c}\right)\left[\frac{1}{2}\frac{x}{x^2+(z+h)^2} + \frac{1}{2}\frac{x}{x^2+(h-z)^2} + k_0 I\right]^{-1}$$
$$\text{at } (x; z=0) \tag{19}$$

where

$$J = \frac{a.c+b.d}{c^2+d^2} - C\pi e^{-k_0(h)}\sin(k_0 x) \tag{20}$$

Next, the effects of finite depth on the lift coefficient of flat-plate and free surface deformations are modeled. The lift coefficient and free surface deformations are determined using the method of images (see Fig. 1) and the following equation for circulation ratio can be obtained as

$$\frac{\Gamma}{\Gamma_\infty}=\left(\frac{\cos\alpha}{c}\right)\left[\frac{1}{2}\frac{x}{x^2+(z+h)^2}+\frac{1}{2}\frac{x}{x^2+(h-z)^2}+k_0 I\right.$$
$$\left.-\frac{1}{2}\frac{x}{x^2+(z+2d-h)^2}-\frac{1}{2}\frac{x}{x^2+(z+2d+h)^2}+k_0 I_{Im}\right]^{-1}$$
$$\text{at}\left(x=\tfrac{c}{2}\cos\alpha,\ \ z=-h-\tfrac{c}{2}\sin\alpha\right)\tag{21}$$

The integral, "I_{Im}" can be written as similar to "I" integral given in Eq. (13)

$$I_{Im}=\int_0^\infty \frac{e^{-k(z+h+2d)}\sin(kx)}{k-k_0}dk\ I_{Im}=\frac{b.c-a.d}{c^2+d^2}+C\pi e^{-k_0(z+h+2d)}\cos(k_0x)\tag{22}$$

Here, C is two (2) for $x\rightarrow+\infty$ and it is zero (0) for $x\rightarrow-\infty$, ensuring satisfaction of the radiation condition given in Eq. (6). The calculated a, b, c and d coefficients are given in the Appendix (Hess and Smith, 1966).

Moreover, the wave elevation on the free surface with the effects of finite depth can be calculated as similar to Eqs. (19) and (20)

$$\frac{\zeta(x;z=0)}{c}=\left(\frac{(\sin\alpha)(\cos\alpha)}{cxK}\right)\left\{I-\frac{1}{2}\frac{1}{ck_0}\left[\frac{2d-h}{x^2+(2d-h)^2}+\frac{2d+h}{x^2+(2d+h)^2}\right]\right\}\tag{23}$$

where

$$K=\frac{x}{x^2+h^2}+k_0I-\frac{0.5x}{x^2+(2d-h)^2}-\frac{0.5x}{x^2+(2d+h)^2}+k_0I_{Im}\tag{24}$$

4. Numerical results

Initially, the method has been validated using results from Plotkin's method (Plotkin 1976), with an angle of attack of $\alpha=5^{o}$ chosen for this verification. As depicted in Fig. 2, the ratios of lift coefficients obtained through the present method demonstrate a very good agreement with those taken from Plotkin's method. When the submergence depth of flat-plate decreases, the influence of the free surface becomes more significant. The effect of the free surface on the lift coefficients of the flat-plate is summarized as follows:

i-) For lower Froude numbers ($Fr=\frac{U}{\sqrt{gc}}$), the presence of the free surface leads to an increase in lift coefficients compared to an unbounded flow domain (without free surface)

ii-) For higher Froude numbers (Fr> 1), there is a decrease compared to the unbounded flow domain (no free surface).

In Fig. 3, the wave elevations using analytical method have been compared wtih those calculated from a previously developed numerical method, known as the Iterative Boundary Element Method (IBEM) (Bal and Kinnas 2002). In IBEM method, a very thin (NACA0002) profile was applied in the calculations. It is worth noting that the differences between the results obtained from the two methods are very close to eachother. In Fig. 4, the relationship between wave elevation and Froude number is depicted for a fixed submergence depth ratio. As the Froude number increases, both the

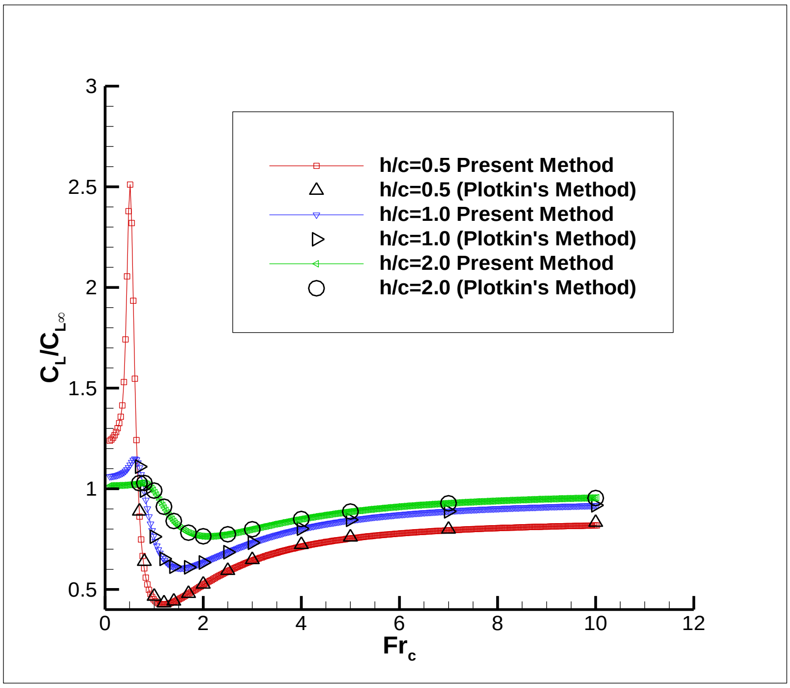

Fig. 2 Variation of lift coefficient ratio versus Froude number at different submergence depths

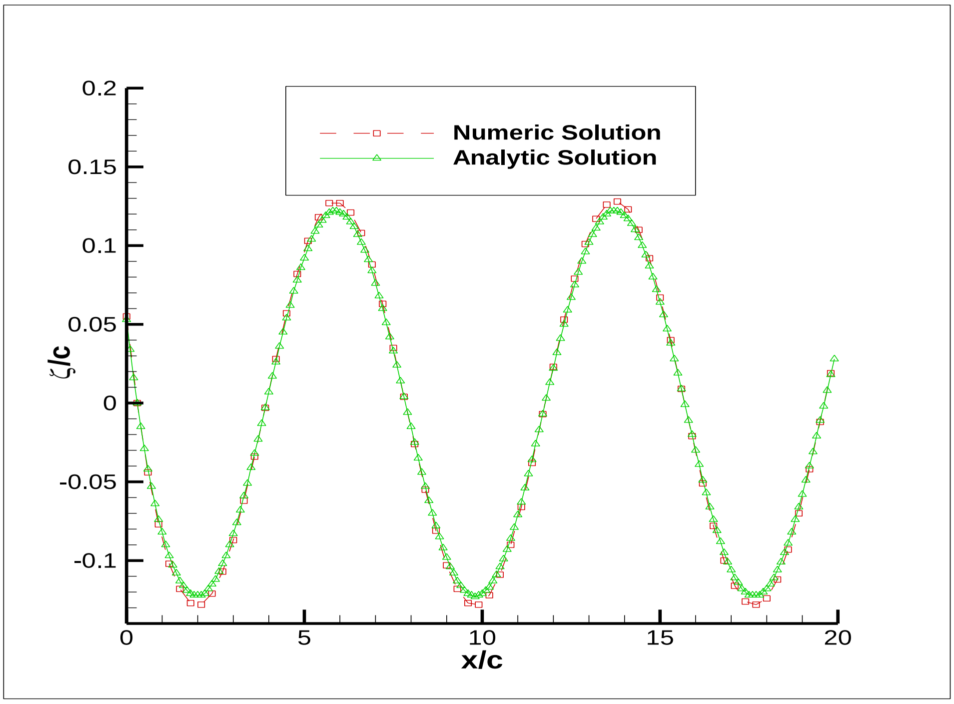

Fig. 3 Comparison of wave elevation with numerical method in deep water, Fr=1.12, α=5°

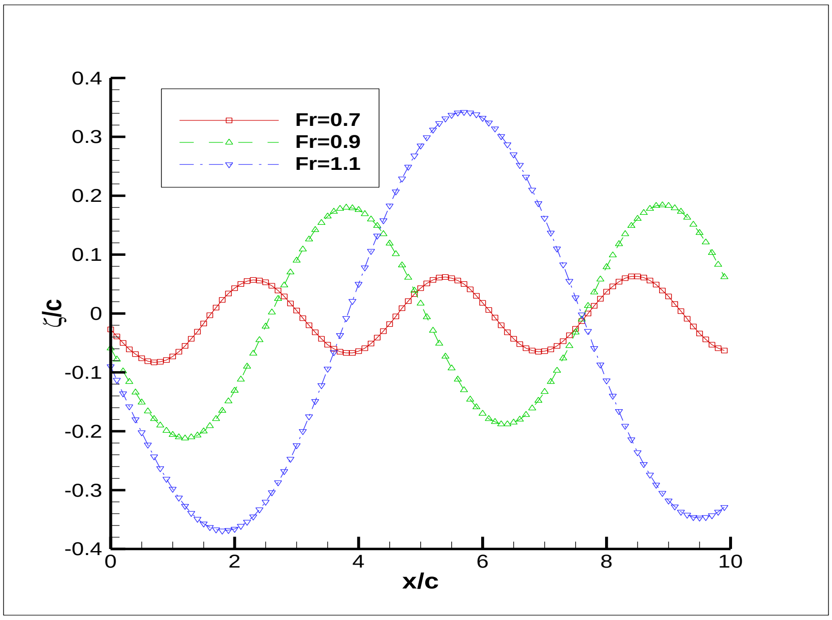

Fig. 4 Variation of wave elevation with Froude number, h/c=1.0, α=5º

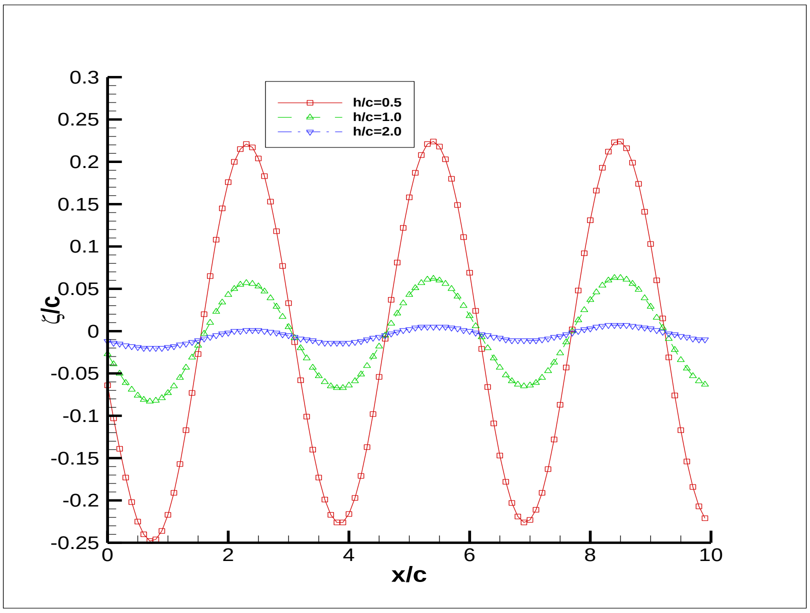

Fig. 5 Variation of wave elevation with submergence depth ratio, Fr=0.7, α=5º

wave height and wave length become larger. Fig. 5 demonstrates the influence of submergence depth on wave elevation while now maintaining a constant Froude number. Notice that as the submergence depth decreases (indicating the flat-plate approaches the free surface), the wave height increases

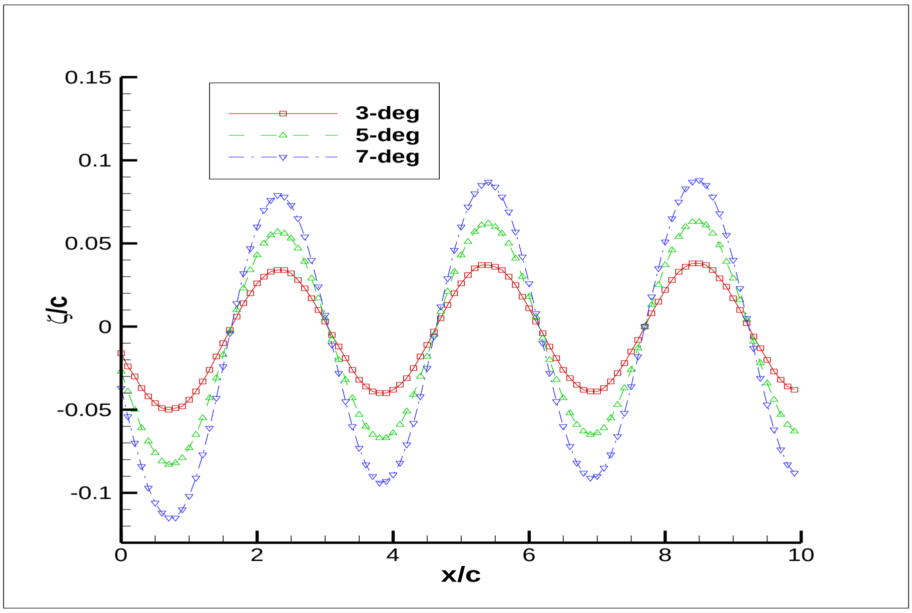

Fig. 6 Angle of attack effect on wave elevation Fr=0.7, h/c=1.0

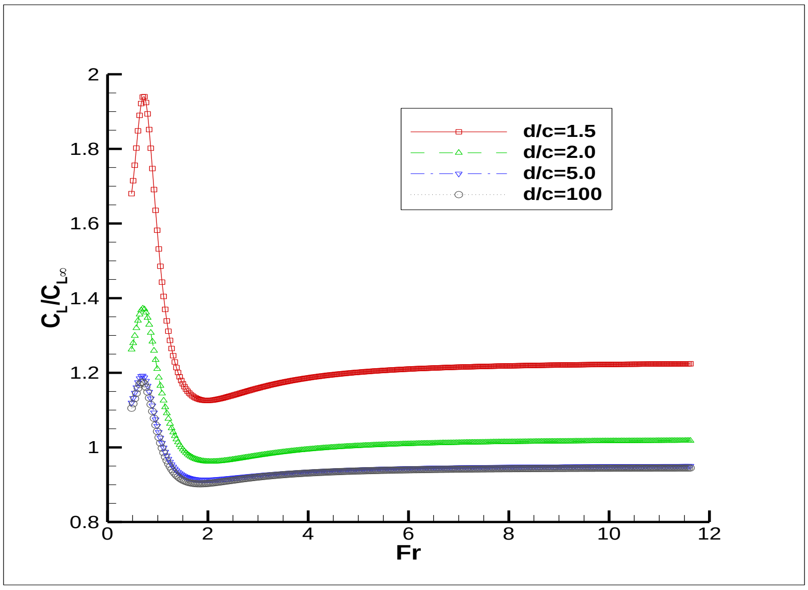

Fig. 7 Angle of attack effect on wave elevation Fr=0.7, h/c=1.0

while the wave length remains unchanged. Fig. 6 illustrates the impact of the angle of attack on wave elevations. Notice also that when the angle of attack increases, while keeping the Froude number and the submergence depth ratio constant, the wave height increases. However, there is no change in the wave length, as it remains constant.

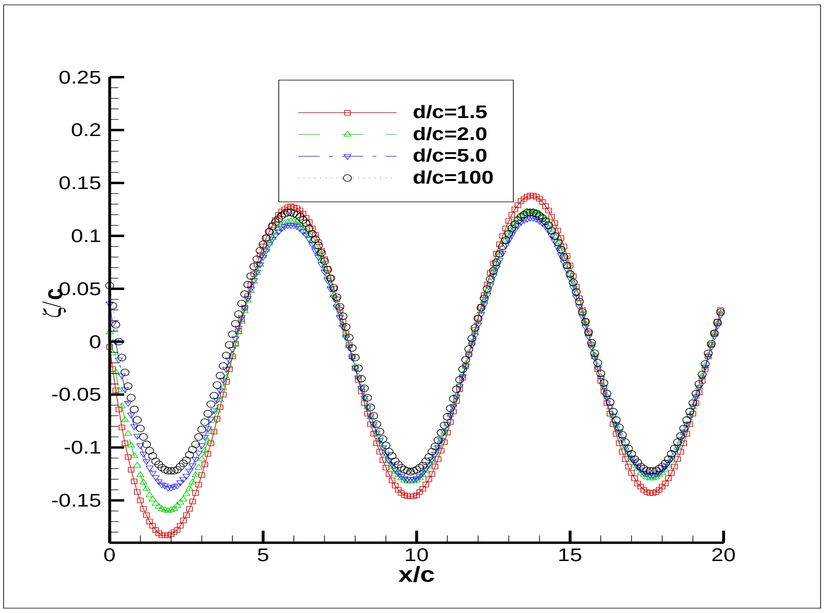

Fig. 8 Variation of wave elevation with depth ratio, Fr=1.12, h/c=1.0, α=5º

Next, the findings related to the effects of finite depth are presented. Fig. 7 shows how the lift coefficient ratios vary with the Froude number at different finite depth ratios. It is observed that the finite depth increases the lift coeffcients at all Froude numbers. In other words, as the depth ratios (d/c) decrease, the loading on flat-plate increases. Figure 8 illustrates the wave elevations at different finite depth ratios for a fixed submergence depth ratio of h/c=1.0 and a fixed Froude number of Fr=1.12. This figure also supports the observation that a decrease in finite depth ratio increases the loading (circulation) on the flat-plate. Note that the wave height increases as the finite depth ratios decrease. The finite depth ratio d/c=100 corresponds to the deep water (infinite depth) case.

5. Conclusions

A hydrodynamic analysis was conducted to examine the lift coefficient of a non-cavitating flat-plate moving at a constant speed under a free surface. Wave deformations due to the flat-plate on the free surface were also calculated. All calculations were based on an analytic approach. The flat-plate was represented by a lumped vortex element, which, to the author's knowledge, has not been previously studied in the literature. The analysis resulted in obtaining closed-form solutions for lift coefficients and wave elevations. The accuracy of the method was confirmed by comparing the results with Plotkin’s method and with an advanced numerical method (IBEM). The following findings were observed:

• The presence of a free surface leads to an increase in the lift coefficients of the flat-plate at lower Froude numbers. However, for higher Froude numbers, (greater than 1), the lift coefficients decrease.
• An increase in Froude number causes an increase in wave height and wave length.
• A decrease in submergence depth ratio from the free surface result in an increase in wave height.
• Increasing the angle of attack for a fixed Froude number and fixed submergence depth from free

surface leads to an increase in wave height, while wave length remains unaffected.
• The finite depth increases the lift coefficient of the flat-plate.
• The finite depth also causes an increse in wave height but not in wave length.

References

Anevlavi, D. and Belibassakis, K.A. (2022), “Analysis of partially cavitating hydrofoils under the free surface using BEM-based adjoint optimization”, *Appl. Math. Model.*, **112**, 415-435. https://doi.org/10.1016/j.apm.2022.07.033.

Anevlavi, D. and Belibassakis, K.A. (2021), “An adjoint optimization prediction method for partially cavitating hydrofoils”, *J. Mar. Sci. Eng*., **9,** 1-18. https://doi.org/10.3390/jmse9090976.

Bai, K.J. and Han, J.A. (1994), “A localized finite-element method for nonlinear steady waves due to a two-dimensional hydrofoil”, *J. Ship Res.*, **58**, 42-51. https://doi.org/10.5957/jsr.1994.38.1.42.

Bal, S., Kinnas, S.A. and Lee, H. (2001), “Numerical analysis of 2-D and 3-D cavitating hydrofoils under a free surface”, *J. Ship Res*., **45**, 34-49. https://doi.org/10.5957/jsr.2001.45.1.34.

Bal, S. (2008), “Prediction of wave pattern and wave resistance of surface piercing bodies by a boundary element method”, *Int. J. Numer. Method. Fl*., **56,** 305-329. https://doi.org/10.1002/fld.1527.

Bal, S. (2011), “The effect of finite depth on 2-D and 3-D cavitating hydrofoils”, *J. Mar. Sci. Technol.*, **16**, 129-142. https://doi.org/10.1007/s0077-011-0117.2.

Bal, S. (2016), “Free surface effects on 2-D airfoils and 3-D wings moving over water”*, Ocean Syst. Eng.,* **6**(6), 245-264. https://doi.org/10.12989/ose.2016.6.245.

Bal, S. and Kinnas, S.A. (2002), “A BEM for the prediction of free surface effect on cavitating hydrofoils”*, Comput. Mech.,* **28**, 260-274. https://doi.org/10.1007/s00466.001.0286.7.

Celik, F., Ozden, Y.A. and Bal, S. (2014), “Numerical simulation of the flow around two-dimensional partially cavitating hydrofoils”, *J. Mar. Sci. Appl.*, **13**, 245-254. https://doi.org/10.1007/s11804.01.1254.x.

Chen, Z.M. (2012), “A vortex-based panel method for potential flow simulation around a hydrofoil”*, J. Fluids Struct*., **28**, 378-391. https://doi.org/10.116/j.jfluidstructs.2011.10.003.

Choi, J.K. and Kinnas, S.A. (1998), “Numerical water tunnel in two and three dimensions”, *J. Ship Res.,* **42**, 86-98. https://doi.org/10.5957/jsr.1998.42.2.86.

Conesa, F.R. and Liem, R.P. (2020), “Slotted hydrofoil design optimization to minimize cavitation in amphibious aircraft application: A numerical simulation approach”, *Adv. Aircraft Spacecraft Sci.*, **7**(4), 309-333. https://doi.org/10.12989/aas.2020.7.4.309.

Hess, J.H. and Smith, A.M.O. (1967), “Calculation of potential flow about arbitrary bodies”, *Progress in Aeronautical Sciences*, **8**, 1-138. https://doi.org/10.1016/076-021(67)9000-6.

Faltinsen, O.M. and Semenov, Y.A. (2008), “The effects of gravity and cavitation on a hydrofoil near the free surface”, *J. Fluid Mech.*, **597**, 371-394. https://doi.org/10.1017/s0022112007009822.

Gradshteyn, I.S. and Ryzhik, I.M. (1965), “Table of integrals, series and products”, Academic Press, USA. https://doi.org/10.1016/C2010-0-64839-5.

Gretton, G.I., Bryden, I.G., Couch, S.J. and Ingram, D.M (2010), “The CFD simulation of a lifting hydrofoil in close proximity to a free surface”, *Proceedings of the* 29*th* *International Conference on Ocean, Offshore and Arctic Engineering*, Shanghai, China, OMAE2010-20936. https://doi.org/10.1115/OMAE2010-20936.

Roohi, E., Zahiri, A.P. and Passandideh-Fard, M. (2013), “Numerical simulation of cavitation around a two-dimensional hydrofoil using VOF and LES turbulence model”, *Appl. Math. Model.*, **37**, 6469-6448. https://doi.org/10.1016/j.apm.2012.09.002.

Karim, Md.M., Prasad, B. and Rahman, N. (2014), “Numerical simulation of free surface water wave for the flow around NACA0015 hydrofoil using the Volume of Fluid (VOF) method”, *Ocean Eng*., **78**, 89-94. https://doi.org/10.1016/j.oceaneng.2013.12.013.

Katz, J. and Plotkin, A. (2001), “Low speed aerodynamics: From wing theory to panel methods”, Cambridge University Press, Cambridge, USA. https://doi.org/10.1017/CB09780511810329.

Katz, J. (2019), “Convergence and accuracy of potential flow methods”, *J. Aircraft*, **56**, 2371-2375. https://doi.org/10.2514/1.C03483.
Kinnas, S.A. (1992), "Inversion of the source and vorticity equations for supercavitating hydrofoils”, *J. Eng. Math*., **26**, 349-361. https://doi.org/10.1007/BF00042728.
Mansoor, W.F., Hocking, G.C. and Farrow, D.E. (2022), “Flow induced by a line sink near a vertical wall in a fluid with a free surface Part I: infinite depth”, *J. Eng. Math.*, **133**, 1-17. https://doi.org/10.1007/s10665-022-10217-8.
Plotkin, A. (1976), “A note on the thin-hydrofoil theory of Keldysh and Lavrenties”, *J. Ship Res*., **20**, 95-97. https://doi.org/10.5957/jsr.1976.20.2.95.
Vrinos, P., Samouchos, K. and Giannakoglou, K. (2021), “The continuous adjointcut-cell method for shape optimization in cavitating flows”, *Comput. Fluids*, **224**, 104974. https://doi.org/10.1016/j.compfluid.2021.104974.
Xie, Z., Liu, Y. and Falzarano, J. (2017), “A more efficient numerical method of the green function in finite water depth”, *Ocean Syst. Eng*., **7**(4), 399-412. https://doi.org/10.12989/ose.2017.7.4.399.
Yu, M. and Falzarano, J. (2017), “A comparison of the Neumann-kelvin and rankine source methods for wave, resistance calculations”, *Ocean Syst. Eng*., **7**(4), 371-398. https://doi.org/10.12989/ose.2017.7.4.371.

MK

Appendix

After the definitions of $r = \sqrt{x^2 + (z - h)^2}$ and $\beta = \tan^{-1}\left(\frac{x}{y-h}\right)$, the following constant hold as given on pages 66-67 of [23]:

$$a = -[\ln(k_0 r) + 0.99999207\gamma + m_1 k_0 r(\ln(k_0 r)\cos\beta - \beta\sin\beta) + \gamma n_1 k_0 r\cos\beta + m_2 {k_0}^2 r^2(\ln(k_0 r)\cos 2\beta - \beta\sin 2\beta) + \gamma n_2 {k_0}^2 r^2\cos 2\beta + m_3 {k_0}^3 r^3(\ln(k_0 r)\cos 3\beta - \beta\sin 3\beta) + \gamma n_3 {k_0}^3 r^3\cos 3\beta + m_4 {k_0}^4 r^4(\ln(k_0 r)\cos 4\beta - \beta\sin 4\beta) + \gamma n_4 {k_0}^4 r^4\cos 4\beta + \gamma n_5 {k_0}^5 r^5\cos 5\beta$$

$$b = -[\beta + m_1 k_0 r(\ln(k_0 r)\sin\beta + \beta\cos\beta) + \gamma n_1 k_0 r\sin\beta + m_2 {k_0}^2 r^2(\ln(k_0 r)\sin 2\beta + \beta\cos 2\beta) + \gamma n_2 {k_0}^2 r^2\sin 2\beta + m_3 {k_0}^3 r^3(\ln(k_0 r)\sin 3\beta + \beta\cos 3\beta) + \gamma n_3 {k_0}^3 r^3\sin 3\beta + m_4 {k_0}^4 r^4(\ln(k_0 r)\sin 4\beta + \beta\cos 4\beta) + \gamma n_4 {k_0}^4 r^4\sin 4\beta + \gamma n_5 {k_0}^5 r^5\sin 5\beta$$

$$c = 1 + d_1 k_0 r\cos\beta + d_2 {k_0}^2 r^2\cos 2\beta + d_3 {k_0}^3 r^3\cos 3\beta + d_4 {k_0}^4 r^4\cos 4\beta + d_5 {k_0}^5 r^5\cos 5\beta + d_6 {k_0}^6 r^6\cos 6\beta$$

$$d = d_1 k_0 r\sin\beta + d_2 {k_0}^2 r^2\sin 2\beta + d_3 {k_0}^3 r^3\sin 3\beta + d_4 {k_0}^4 r^4\sin 4\beta + d_5 {k_0}^5 r^5\sin 5\beta + d_6 {k_0}^6 r^6\sin 6\beta$$

γ=0.5772156649

m_1=0.23721365, m_2=0.0206543, m_3=0.000763297, m_4=0.0000097687

n_1=-1.49545886, n_2=0.041806426, n_3=-0.03000591, n_4=0.0019387339, n_5=-0.00051801555

d_1=-0.76273617, d_2=0.28388363, d_3=-0.066786033, d_4=0.012982719, d_5=-0.0008700861, d_6=0.0002989204

Nomenclature

c	: Chord length
C_L	: Lift coeffcicient
$C_{L\infty}$	: Lift coeffcicient
d	: Depth of finite bottom from free surface
Fr	: Froude number
g	: Gravitational acceleration
h	: Submergence depth of flat-plate from free surface
k_0	: Wave number
L	: Lift force
U	: Uniform inflow velocity
x	: Horizontal coordinate
z	: Vertical coordinate
α	: Angle of attack
Γ	: Circulation
Γ_∞	: Circulation in unbounded flow domain
$\boldsymbol{\phi}$	: Perturbation potential
Φ	: Total potential
ρ	: Density of water
ζ	: Wave elevation